ARCHIVES
OF THERMODYNAMICS

Finite element analysis of femur bone fracture – modelling and analysis

Pranjal Sarmah[a], Ravi Kumar[a], Amrit Thakur[a], Mohit Sharma[a],
Surendra Kumar Yadav [b*], Virendra Kumar[c*]

[a]Department of Mechanical Engineering, Dibrugarh University, Dibrugarh 786004, Assam, India
[b]Department of Mechanical Engineering, K. R. Mangalam University, Gurugram 122001, India
[c]Department of Mechanical Engineering, Harcourt Butler Technical University, Kanpur 208002, India
*Corresponding author email: s.k.yadav86@gmail.com, virendra.k@hbtu.ac.in

Abstract

Femoral fractures are frequent in adolescents and children, and most fractures occur within the centre of the bone, typically referred to as the femur shaft. Plate and screws are ideal fixation methods for femoral fractures close to the articular surfaces. When using plates and screws, estimating the load on the plates and screws before starting treatment is important. The primary focus of this paper is the examination of fixation plates utilized in the treatment of femur bone fractures. The study employs the finite element method to conduct this analysis. Initial modelling of the femur bone is executed through the utilization of CATIA V5 software. Subsequently, the investigation transitions to the ANSYS R14.5 environment, where more in-depth analysis is carried out. The modelling of the fracture fixation plates is done on commercially available CAD software CATIA V5. The stress distribution of different biomaterials in the bone plate system is calculated when the system is subjected to compressive loads with varying healing times. Here we have used stainless steel (SS316-L), titanium alloy (Ti6Al4V) and magnesium alloy (AZ31). More focus was given to the magnesium alloy. Here a fracture gap of 1mm gap was taken for analysis. A comprehensive compressive force amounting to 750 N was applied to the bone-plate assembly during the simulation. This force magnitude corresponds to the approximate weight of an average human body.

Keywords: Femur shaft; Simulation; Fixation plate; Finite element method.

1. Introduction

Biomechanics is the branch of science that uses mechanical principles concerning all forces acting on the human body and the effects of the forces on the bone to analyse the biological system. It is a branch of science that deals with applying mechanical principles to biological things [1]. The biomechanical elements that determine the rate of healing efficiency of a fractured bone treated with plates and screws are given to the fractured bone in the form of (a) the level of bone contact that occurs at the fracture interface and (b) stability provided to the fractured bone in terms of reduced motion at the fracture interface, and (c) Necessary and adequate stress shielding of bone at and away from the fracture interface [2]. Studied ways to accurately predict the strength and risk of fractures in femurs with metastases using finite element modelling. However, there's a variety in the material models, loading conditions, and critical thresholds used in these models [3]. Orthopaedic surgeons are finding it challenging to treat bone fractures resulting from accidents. To address this issue, screws and locking compression plates are used

to externally stabilize fractured bones. In this study, we modelled the femur bone, locking compression plate, and screws. We then analysed the existing materials for joining plates using different materials [4]. Bones serve as the body's main structural support, protecting vital organs and giving us a sturdy frame for movement. Studying bone mechanics helps us understand how and why bones break. From an engineering perspective, fractures happen when the force or pressure on a bone exceeds its capacity to bear the load [5]. Bones are crucial tissues made of calcium and phosphorus. They grow quickly in their early years and repair themselves well. Bones are essential for the human skeleton, providing support for the softer parts of the body. When bones crack, a common way to treat them is by using bone joints to reconnect the broken parts [6].

The term "femur bone" pertains to a bone-like substance that is synthesized within a laboratory setting. This material finds application in bone graft procedures, serving as a replacement for human bone loss resulting from conditions such as severe fractures, illnesses, and related factors [6]. The femur bone stands as the longest and most robust bone within the human body, bridging the connection between the hip joint and the knee joint. [7]. The femur bone contains a linear elastic, isotropic and homogenous material of calcium phosphate. In the human body during static loading, femur bone supports weight in between the hip and knee joints. In femur mid shaft fracture is common [8]. It fractures due to the sudden impact of a large amount of force, for example accidents, fall from great height. In some cases, due to osteoporosis small amounts of force can also fracture the femur bone. To promote bone structure stabilisation, various types of internal fixation devices like bone plates are used [9]. The femur bone can bear 25% of the body weight of the person's height. It can bear 2 500 N force (which is 4 times the body weight) without any significant change in the factor of safety [10]. Figures 1 and 2 show the complete structure of the femur bone and the cut section of the bone respectively. The material properties of cortical and trabecular bone are shown in Tables 1 and 2, respectively.
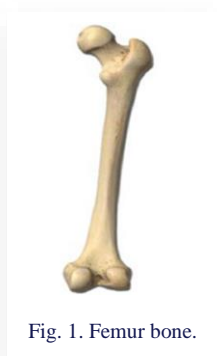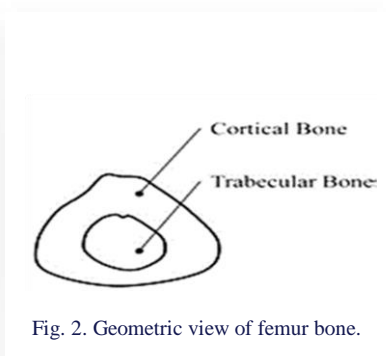

Fig. 1. Femur bone.

Fig. 2. Geometric view of femur bone.

Biomaterials are used in the manufacture of structures to replace broken or diseased biological structures or parts and restore their morphology and function. Biomaterials interact with cells and exhibit stereotypical responses. Biomaterials have to show bio-functionally and bio-compatibility properties. Biodegradable materials can get decomposed by the action of microorganisms such as bacteria. When considering biomedical uses,

the choice of a biodegradable material becomes a pivotal aspect. This decision bears weight due to the material's density, mechanical characteristics, and rates of corrosion (biodegradation), all of which notably influence both the implant plate's design and its performance [11]. Over the span of the last six decades, substantial progress has been made in the development of novel materials characterized by excellent biocompatibility. This evolution encompasses three distinct generations: the initial generation marked by bioinert materials, the subsequent generation featuring bioactive and biodegradable materials, and the most recent third generation characterized by biologically adaptive materials [12].

Table 1. Material properties of cortical bone [19].

No.	Parameters	Value
1	Material	Cortical bone
2	Elastic modulus	16 700 MPa
3	Density	1 750 kg/m³
4	Poisson's ratio	0.26

Table 2. Material properties of trabecular bone [19].

No.	Parameters	Value
1	Material	Trabecular bone
2	Elastic modulus	100 MPa
3	Density	1 750 kg/m³
4	Poisson's ratio	0.3

A new era has dawned in the realm of developing implant materials that are both corrosion-resistant and biodegradable, tailored to harmonize with the physiological milieu. The imperative is for these implant materials to satisfy specific mechanical requisites, enabling them to effectively endure biomechanical forces. Implant materials that were used in this study are titanium alloy, stainless steel alloy and magnesium alloy. Research says that the best-suited material for orthopaedic implants is Magnesium alloy because of its biocompatibility, biodegradability, bioresorbable, closer density, Young modulus of bone (E = 10−30 GPa), low-stress shielding effect, and light in weight. The strain distribution of the callus generated between the fractured surfaces was considered the main criterion in determining the best bone plate performance. A connected study by [8,13] found that a gap strain of 2% to 10% was effective in creating and developing callus at the fracture site by stimulating healing tissue. Callus is also known to develop dramatically 4−8 weeks after surgery, which is generally considered to be the most important time for fracture healing [14−16]. The material properties of callus are shown in Table 3.

Fracture fixation can also be accomplished through secondary-type healing via callus formation, which takes place when new bone is produced at the location of the fracture site and its porosity is reduced as it develops into a mature structure. Inflammation, soft callus, hard callus, and bone remodelling are the four steps that take place, and during each stage, the mechanical stiffness and strength increase [17].

Table 3. Material properties of callus [21].

No.	Property	Callus 1%	Callus 50%	Callus 100%
1	Density (kg/m³)	1 100	1 500	1 750
2	Elastic modulus E (MPa)	20	10 000	16 700
3	Poisson's ratio	0.3	0.3	0.3

Table 4. Material properties of Mg alloy [20].

No.	Parameters	Value
1	Material	Mg Alloy (AZ31)
2	Elastic modulus	45 000 MPa
3	Density	1 810 kg/m³
4	Poisson's ratio	0.35
5	Shear modulus	16.67 GPa
6	Ultimate tensile strength	260 MPa

Table 5. Material properties of Ti-6Al-4V alloy [21].

No.	Parameters	Value
1	Material	Ti-6Al-4V Alloy
2	Elastic modulus	120 000 MPa
3	Density	4 500 kg/m³
4	Poisson's ratio	0.32
5	Shear modulus	45 455 MPa
6	Ultimate tensile strength	397.2 MPa

Table 6. Material properties of SS316-L alloy [18].

No.	Parameters	Value
1	Material	SS316L Alloy
2	Elastic modulus	193 000 MPa
3	Density	7 750 kg/m³
4	Poisson's ratio	0.31
5	Shear modulus	73 664 MPa
6	Ultimate tensile strength	570 MPa

Hence, it holds significance to offer the optimal gap or load on the callus during this phase. Upon completion of an eight-week healing interval, the callus reaches a state conducive to the formation of solid bone, heightening the importance of stabilizing the fractured site. This study aimed to explore the biomechanical viability of bone plates constructed from diverse biomaterials, aiming to establish an environment conducive to the effective development of callus.

2. Method: finite element method

The finite element analysis is a practical implementation of the finite element method, utilized to carry out detailed assessments through this methodology. To check developed structural stresses finite element analysis (FEA) is used. It also helps in identifying high-stress zones in implant design. Solid models of implant material such as bone plates and screws were created in CATIA software. The completed assembly was transferred to the ANSYS Workbench program for finite element analysis, with the export facilitated through the utilization of CATIA V5 software.

The Finite Element Method is a numerical approach used to get an approximate solution to problems such as boundary values using elliptical partial differential equations. Because the finite element approach transforms these elliptical partial differential equations into a set of algebraic equations, they are easily solved. FEA additionally establishes a correlation between the quantity of elements employed and the level of analytical accuracy achieved.

2.1. Selection of material and methodology

Biological internal fixation has no effect on early and complete restoration of bone, limb and patient function, but recognition of optimal requirements for bone healing is now preferred, with stable performance and less rigid mechanics while still allowing painless and reliable functional healing [13]. The biomaterials that are selected for this study are:
- Magnesium Alloy (AZ31), Table 4,
- Titanium (Ti-6Al-4V Alloy), Table 5,
- Stainless steel (SS316L Alloy), Table 6.

Here Table 4 represents the material properties of Mg Alloy, Table 5 represents the material properties of Ti-6Al-4V Alloy and Table 6 represents the material properties of SS316-L Alloy, respectively. Complete material properties along with the data showing the elastic modulus, shear modulus, density, and Poisson's ratio are represented in the tables below respectively. These materials are selected based on their metal compatibility, corrosion, strength and ductility.

Ti-6Al-4V is low-density material. So, it is used for implantation. Because of this, the patient can move his/her leg easily [18]. This alloy has excellent bio-compatibility and mechanical properties. Compared to Ti-alloy stainless steel is more economical. It has poor fatigue strength. Magnesium alloy is biodegradable. It has a low shielding effect and is light in weight.

3. CFD modelling

Within the scope of the finite element simulation, the configuration of the fractured long bone is portrayed as a pair of uniform hollow cylindrical structures, each measuring 280 mm in length and possessing an external diameter of 27 mm. Additionally, solid cylindrical forms with a length of 280 mm and an internal diameter of 13 mm are employed. For the analytical phase, a straightforward transverse fracture pattern, classified as a low-energy fracture, was chosen. The process encompassed the creation of bone and plate models through CATIA V5 software, followed by the assembly of distinct components. The length of the bone plates measures 145 mm, encompassing 8 holes, each featuring a diameter of 4.5 mm. These plates are affixed to the fractured bone using 8 implant alloy screws, each measuring 4.5

mm in diameter and 31 mm in length [8]. Figure 3 shows the geometry (3D models) of the femur bone, plates, and screw which are made in the CATIA software.
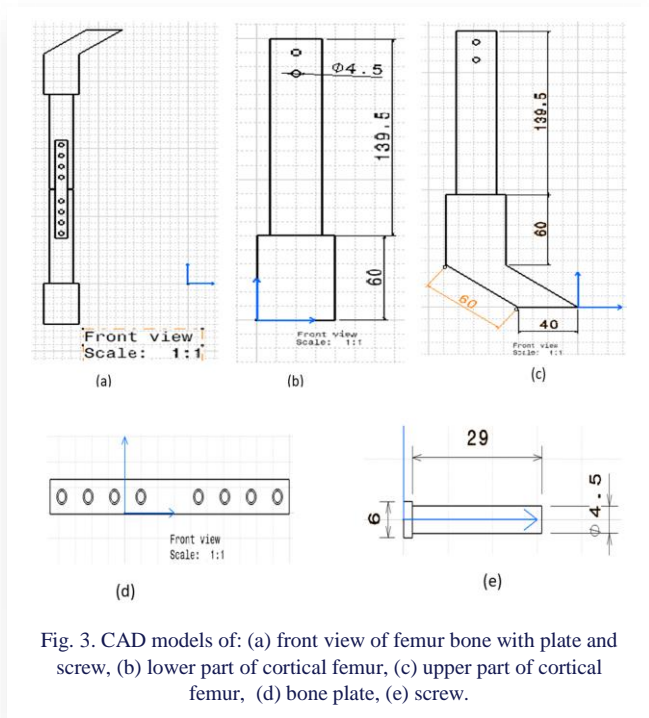

Fig. 3. CAD models of: (a) front view of femur bone with plate and screw, (b) lower part of cortical femur, (c) upper part of cortical femur, (d) bone plate, (e) screw.

Meshing: A mesh is defined as the process of dividing an entire component into a set of elements so that the load is evenly distributed each time the component is loaded. This is called a meshing. Components are analysed in two ways. One is meshed and the other is without meshed.

With Meshing: When a load is applied to a structure or body and the bodies are considered interlocked, the load is evenly distributed throughout the structure. After creating the mesh, the entire structure is divided into several elements, each of which has its stiffness under load.

Without Meshing: Applying loads to bodies in which mesh is not created can result in uneven load distribution and irregular or false results.

In our study, we used ANSYS Workbench R14.5 software to generate a mesh of the femur assembly model, as shown in Fig. 4. We used tetrahedral elements (5 mm) of the same size and shape for the meshing [16,21,22].
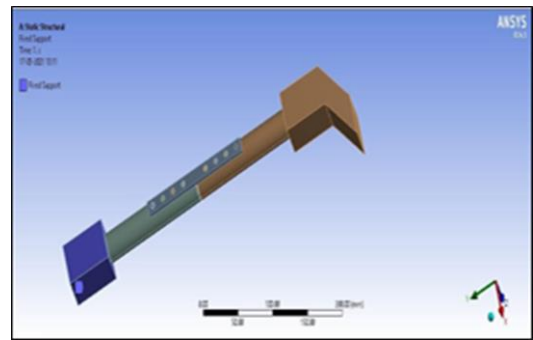

Fig. 4. Meshed model.

3.1. Loading and boundary conditions

A comprehensive compressive force amounting to 750 N was imposed on the cortical region of the femoral head within the assembly. The opposing side of the bone was maintained as a fixed support, resulting in a statically loaded model [20]. The implant plate should exhibit homogeneity, maintaining consistent mechanical and degradation characteristics throughout. The loading conditions for the implant plate are contingent on the two segments of the fractured bone. The fractured lower section of the bone is regarded as anchored by the lower limbs (legs). This signifies that one side of the lower segment can be treated as fixed, secured in place with a screw. Conversely, the upper part of the fractured bone is immobilized, and the upper section of the plate is affixed with screws to withstand the applied load [11]. Figure 5 shows how the assembly is kept in a fixed support from one end and Fig. 6 shows that a load is applied on the assembly from one end.

Fig. 5. Fixed support on assembly.
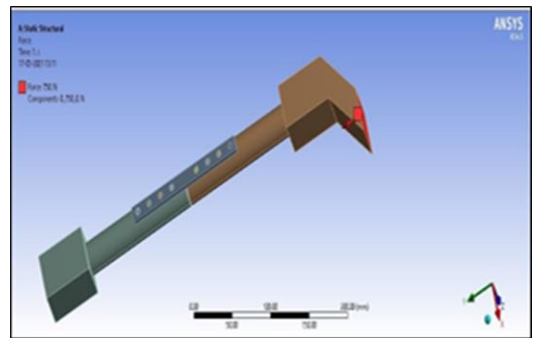

Fig. 6. Load on assembly.
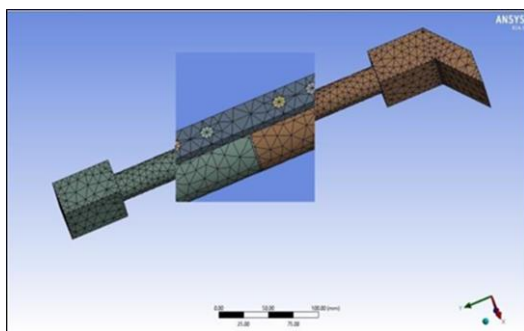
4. Results and discussion

This investigation aimed to assess the levels of maximum and minimum stress, as well as maximum and minimum strain and deformation, resulting from the utilization of implants composed of different materials in a male individual weighing 75 kg, under standard anatomical conditions. The main fluctuations occurring in callus, are 1% and 50%. 100% of the healing phase is achieved with different implant materials and results for each category are calculated. Initially, at around 1%, there is minimal callus formation, characterized by soft fibrous tissue. As the

healing progresses, typically peaking around 50%, the callus transforms into a more rigid structure incorporating both cartilage and woven bone. This intermediate callus provides initial stability to the fractured site. Finally, at 100% the callus undergoes further remodelling, transitioning into mature, lamellar bone. This phase ensures the restoration of strength and function to the bone.

Here, the model was just statically loaded. The following Figures show the response of the bone plate system for a 1 mm gap compressive load using a variety of implant materials. Be-

low Figs 7, 8 and 9 show the Von Mises stress distributions on the bone plate at 1%, 50%, and 100% callus for Ti-6Al-4V alloy. Figures 10−12 show the Von Mises stress distributions on the bone plate at 1%, 50%, and 100% callus for Mg AZ31 alloy. Figures 13−15 show the Von Mises stress distributions on the bone plate at 1%, 50%, and 100% callus SS316-L alloy. Figures 16−18 show the equivalent strain results for Ti-6Al-4V alloy, Mg AZ31 alloy, and SS316-L alloy respectively. Figures 19−21 show the Total deformation results for Ti-6Al-4V alloy, Mg AZ31 alloy, and SS316-L alloy respectively.
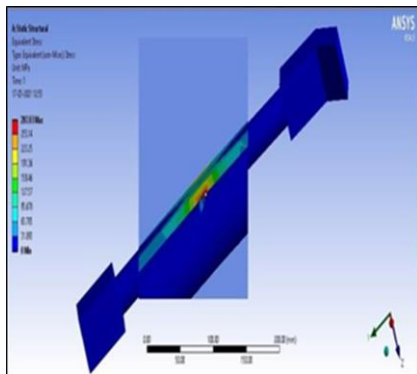

Fig. 7. Von Mises stress distributions on bone plate at 1% callus for Ti-6Al-4V alloy.
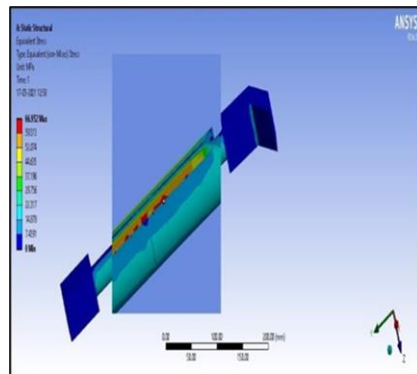

Fig. 8. Von Mises stress distributions on bone plate at 50% callus for Ti-6Al-4V alloy.
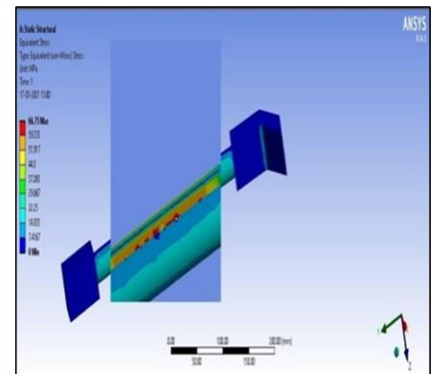

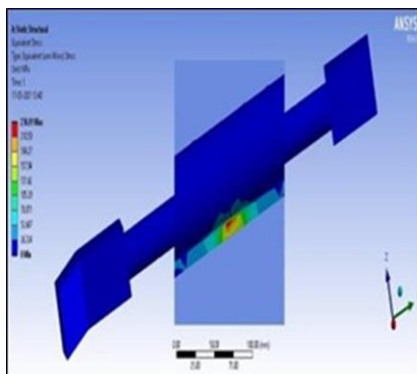Fig. 9. Von Mises stress distributions on bone plate at 100% callus for Ti-6Al-4V alloy.

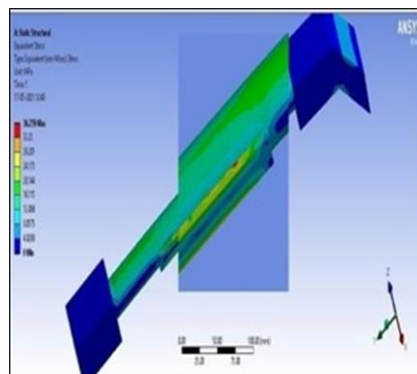Fig. 10. Von Mises stress distributions on bone plate at 1%, callus for Mg AZ31 alloy.

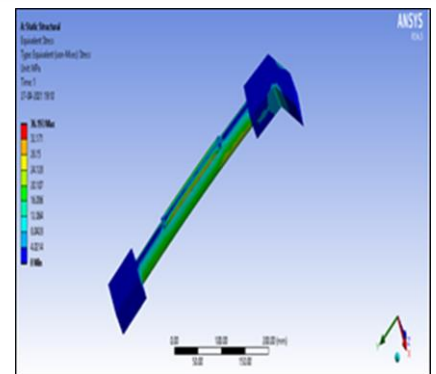Fig. 11. Von Mises stress distributions on bone plate at 50%, callus for Mg AZ31 alloy.

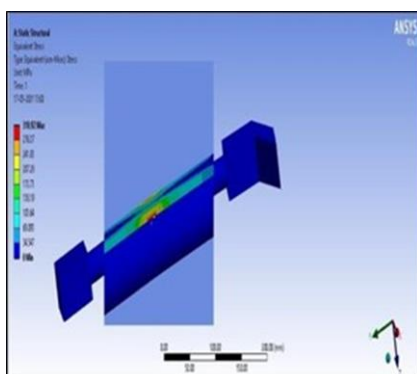Fig. 12. Von Mises stress distributions on bone plate at 100%, callus for Mg AZ31 alloy.

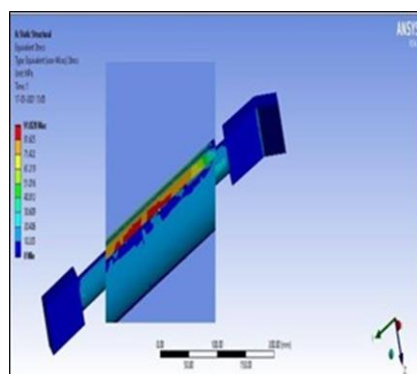Fig. 13. Von Mises stress distributions on bone plate at 1% callus SS316-L alloy.

Fig. 14. Von Mises stress distributions on bone plate at 50% callus SS316-L alloy.
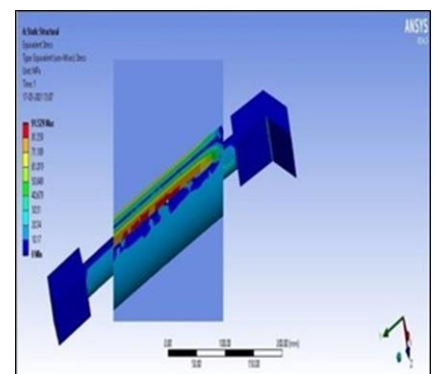

Fig. 15. Von Mises stress distributions on bone plate at 100% callus SS316-L alloy.
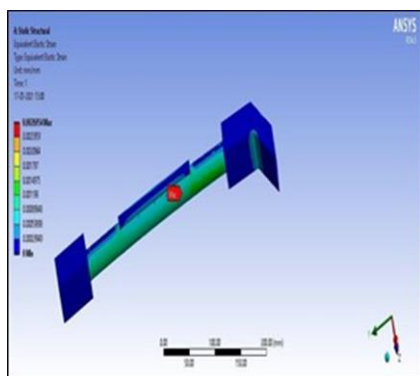
Fig. 16. Equivalent strain results
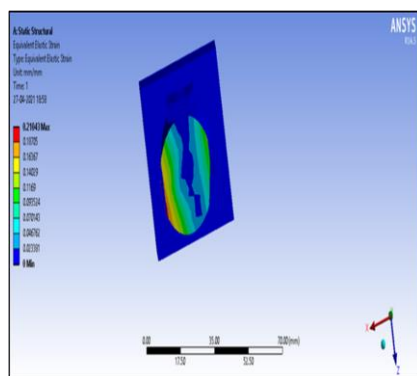for Ti-6Al-4V alloy.

Fig. 17. Equivalent strain results
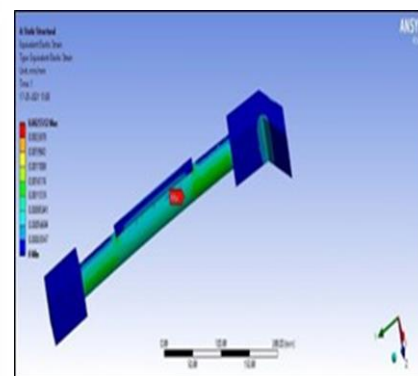for Mg AZ31 alloy.

Fig. 18. Equivalent strain results
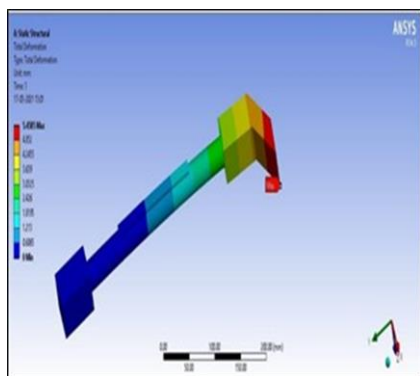for SS316-L alloy.

Fig. 19. Total deformation results
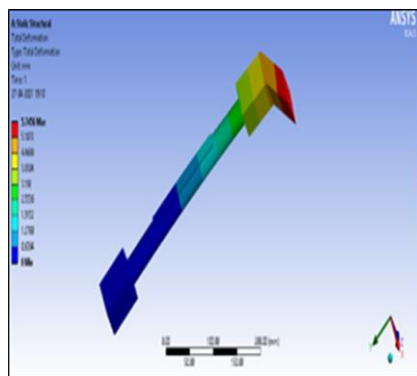for Ti-6Al-4V alloy.

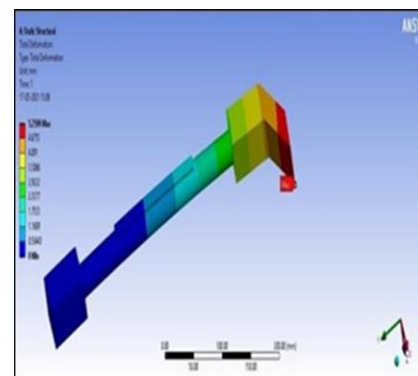
Fig. 20. Total deformation results
for Mg AZ31 alloy.

Fig. 21. Total deformation results
for SS316-L alloy.

Since the fracture zone is immature compared to normal bone tissue, it is not possible to load the bone in the early stages of healing, so the load-bearing part includes only the bone plate. Callus has a low elastic modulus and cannot withstand the load. Therefore, the tension of the bone plate is also relatively higher in the magnesium plate. As the healing duration extends, the fracture zone gains increased strength in contrast to its initial healing phase, thus enabling enhanced load transmission to the bone. During the 50% and 100% healing stages, supplementary callus forms at the fracture junction, affording the bone greater load-bearing capacity. Consequently, the bone and plate function as a composite material, leading to heightened stress levels at the fracture location while concurrently alleviating stress on the bone plate. Figure 22 shows the Graphical representation of obtained stress results with different healing conditions using the three different implant materials which are Mg (AZ31) alloy SS316L alloy and Ti6Al-4V alloy.

In this study, the biomechanical performance of titanium alloys (Ti6Al4V), stainless steel (SS316L), and magnesium alloys used to heal femoral fractures is investigated through finite element analysis. The titanium alloy, stainless steel, and magnesium alloy implants are taken for analysis, various models of the assembly are designed on CATIA software, and the analysis is performed with Ansys R14.5. Previous studies have shown that Magnesium alloys are used in the field of orthopaedics because of their biodegradability, bioabsorbable, Young's modulus of

bone (E = 10 GPa to 30 GPa), less stress shielding effect, and light in weight. It can be seen from Table 7, that the minimum stress that is obtained at various stages of callus formation is in the magnesium alloy. From the results, it is clear that at 1% callus, the value of Von-misses stress of magnesium implant is 236.91 MPa at 50% callus is 36.295 MPa and at 100% callus formation is 36.209 MPa. Therefore, if a fracture occurs in the femoral shaft of the femur, the magnesium alloy plate has the lowest stress compared to other implant materials and can be healed early with a magnesium implant.
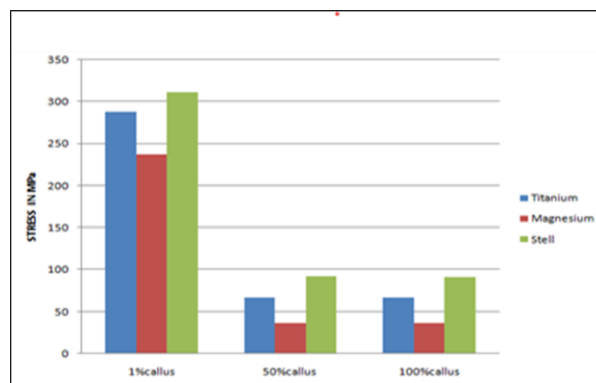

Fig. 22. Graphical representation of obtained stress results
with different healing conditions.

Table 7. Finite element analysis (FEA) results for different bone plate material at different healing conditions (1%, 50%,100% callus).

Name of materials	Stress (MPa)			Strain			Deformation (mm)			LHV
	1%	50%	100%	1%	50%	100%	1%	50%	100%	[%]
Mg (AZ31)	236.91	36.259	36.209	0.23214	0.002899	0.00289	8.6621	5.76	5.75	4272
SS316L	310.92	91.828	91.529	0.12244	0.002556	0.00255	6.2695	5.26	5.25	24402
Ti6Al-4V	287.03	66.952	66.75	0.15242	0.002701	0.00269	6.9585	5.46	5.45	12960

Also, we can say that the stress rating of stainless steel (SS316L) is maximum. Therefore, if a fracture occurs, the stress generated by this implant is maximized at various stages of callus formation and should be avoided. This will take longer for the bone to heal and one can use magnesium or titanium instead. The other two implants are less than when using stainless steel. This is because it leads to better early healing of the fractured bone. And results of this analysis are then displayed in a graph showing the changes in the callus of different implant materials under load. By referring to the figures showing the values of the stress as the load changes when different implant materials being used, the surgeon understands that a better and earlier healing process is achieved when the implant material is used.

5. Conclusions

The test results obtained here provide an insight into the stresses achieved by varying the callus formation. More focus was paid to the stresses on the bone plate assembly. From the results, it is seen that the least stress is obtained in the bone plate assembly of magnesium alloy as compared to other implants. At 100% healing condition, the bone and plate act as a composite material i.e. at 100% healing condition the scar tissue becomes strong hence at the fracture zone it can bear a maximum load, which means if at the callus zone, maximum load is being transferred it means that at fracture zone also maximum stress takes place and it is in a completely healing condition which in turn will result in better bone remodelling.

In our analysis, it is seen that using Mg alloy at 100% callus formation or completely healing conditions minimum stress is obtained in the bone plate assembly as compared to titanium alloy and stainless-steel alloy. Hence at the fracture zone, it will result in maximum stress, and hence Mg alloy will show better bone healing. Also, it is seen that at 1% healing condition of magnesium alloy, 23% strain is not possible. Generally, load sharing should be there but not excess which results in the effect of callus. Also, as time passes by strain should not be high as it will result in slow bone healing and bone fractured bone mass will result in misalignment. New research can be done on strain analysis using different implant materials.

References

[1] Yousif, A.E., & Aziz M.Y. (2012). Biomechanical Analysis of the human femur bone during normal walking and standing up. *IOSR Journal of Engineering*, 2(8), 13–19. doi: 10.9790/3021-02851319

[2] Ganesh, V.K., Ramakrishna, K., & Ghista, D.N. (2005). Biomechanics of bone-fracture fixation by stiffness-graded plates in comparison with stainless-steel plates. *Biomedical Engineering*, 4(1), 46. doi: 10.1186/1475-925x-4-46

[3] O'Rourke, D., Johnson, L.J., Jagiello, J., & Taylor, M. (2023). Examining agreement between finite element modelling methodologies in predicting pathological fracture risk in proximal femurs with bone metastases. *Clinical Biomechanics (Bristol, Avon)*, 104, 105931. doi: 10.1016/j.clinbiomech.2023.105931

[4] Balasubramani, V., Gokul, D., & Gokul, R.K. (2023). Modelling and finite element analysis of fractured femur bone with locking compression plate under fatigue load condition. *Materials Today: Proceedings*. doi: 10.1016/j.matpr.2023.03.437

[5] Manubolu, V.N., & Reddy, D. (2022). Design aspects of femur bone fractures: A review. *Materials Today: Proceedings*, 68(6), 2676–2681. doi: 10.1016/j.matpr.2022.09.558

[6] Kalaiyarasan, A., Sankar, K., & Sundaram, S. (2020). Finite element analysis and modeling of fractured femur bone. *Materials Today: Proceedings*, 22(3), 649−653. doi: 10.1016/j.matpr.2019.09.036

[7] Manral, A.R., Gariya, N., & Kumar, K N. (2020). Material optimization for femur bone implants based on vibration analysis. *Materials Today: Proceedings*, 28(4), 2393−2399. doi: 10.1016/j.matpr.2020.04.714

[8] Fang, R., Ji, A., Zhao, Z., Long, D., & Chen, C. (2020). A regression orthogonal biomechanical analysis of internal fixation for femoral shaft fracture. *Biocybernetics and Biomedical Engineering*, 40(3), 1277−1290. doi: 10.1016/j.bbe.2020.07.006

[9] Fouad, H.J. (2011). Assessment of function-graded materials as fracture fixation bone-plates under combined loading conditions using finite element modelling. *Medical Engineering & Physics*, 33(4), 456−463. doi: 10.1016/j.medengphy.2010.11.013

[10] Innocenti, B., Bellemans, J., & Catani, F. (2016). Deviations from optimal alignment in TKA: Is there a biomechanical difference between femoral or tibial component alignment? *The Journal of Arthroplasty*, 31(1), 295−301. doi: 10.1016/j.arth.2015.07.038

[11] Chandra, G., Pandey, A., & Pandey, S. (2020). Design of a biodegradable plate for femoral shaft fracture fixation. *Medical Engineering & Physics*, 81, 86−96. doi: 10.1016/j.medengphy.2020.05.010

[12] Cheng, C.K., Wang, X.H., Luan, Y.C., Zhang, N.Z., Liu, B.L., Ma, X.Y., & Nie, M.D. (2019). Challenges of pre-clinical testing in orthopedic implant development. *Medical Engineering & Physics*, 72, 49−54. doi: 10.1016/j.medengphy.2019.08.006

[13] Perren, S.M. (2002). Evolution of the internal fixation of long bone fractures: The scientific basis of biological internal fixation: Choosing a new balance between stability and biology. *The Journal of Bone and Joint Surgery. British Volume*, 84-B(8), 1093−1110. doi: 10.1302/0301-620X.84B8.0841093

[14] Kim, S.H., Chang, S.H., & Jung, H.J. (2010). The finite element analysis of a fractured tibia applied by composite bone plates considering contact conditions and time-varying properties of curing tissues. *Composite Structures*, 92(9), 2109−2118. doi: 10.1016/j.compstruct.2009.09.051

[15] Gardnera, T.N., Stoll, T., Marks, L., Mishra, S., & Tate, M.K. (2000). The influence of mechanical stimulus on the pattern of tissue differentiation in a long bone fracture − an FEM study.

Journal of Biomechanics, 33(4), 415−425. doi: 10.1016/S0021-9290(99)00189-X

[16] Izzawati, B., Daud, R., Rojan, A., Majid, M.A., Najwa, M.N., Zain, N.A., & Azizan, A.F. (2019). The effect of bone healing condition on the stress of screw fixation in orthotropic femur bone for fracture stabilization. *Materials Today: Proceedings*, 16(4), 2160−2169. doi: 10.1016/j.matpr.2019.06.106

[17] Samiezadeh, S., Schemitsch, E. H., Zdero, R., & Bougherara, H. (2020). Biomechanical response under stress-controlled tension-tension fatigue of a novel carbon fiber/epoxy intramedullary nail for femur fractures. *Medical Engineering & Physics*, 80, 26−32. doi: 10.1016/j.medengphy.2020.04.001

[18] Amalraju, D., & Dawood, A.K. (2012). Mechanical strength evaluation analysis of stainless steel and titanium locking plate for femur bone fracture. *Engineering Science and Technology: An International Journal*, 2(3), 381−388.

[19] Dhason, R., Roy, S., & Datta, S. (2020). A biomechanical study on the laminate stacking sequence in composite bone plates for vancouver femur B1 fracture fixation. *Computer Methods and Programs in Biomedicine*, 196, 105680. doi: 10.1016/j.cmpb.2020.105680

[20] Kumar, K.N., Griya, N., Shaikh, A., Chaudhry, V., & Chavadaki, S. (2020). Structural analysis of femur bone to predict the suitable alternative material. *Materials Today: Proceedings*, 26, 364−368. doi: 10.1016/j.matpr.2019.12.031

[21] Das, S., & Sarangi, S.K. (2014). Finite element analysis of femur fracture fixation plates. *International Journal of Basic and Applied Biology*, 1(1), 1−5.

[22] Steiner, L., Synek, A., & Pahr, D.H. (2021). Femoral strength can be predicted from 2D projections using a 3D statistical deformation and texture model with finite element analysis. *Medical Engineering & Physics*, 93, 72−82. doi: 10.1016/j.medengphy.2021.05.012